



Honeycomb membranes prepared from 3-*O*-amino acid functionalized cellulose derivatives

William Z. Xu, Batia Ben-Aroya Bar-Nir, John F. Kadla*

Advanced Biomaterials Chemistry Laboratory, University of British Columbia, Vancouver, BC V6T 1Z4, Canada

ARTICLE INFO

Article history:

Received 13 June 2012

Received in revised form

21 November 2012

Accepted 27 December 2012

Available online 18 January 2013

Keywords:

Cellulose

Regioselective

Poly(ethylene glycol)

3-*O*-Poly(ethylene

glycol)-2,6-di-*O*-thexyldimethylsilyl

cellulose

Honeycomb

ABSTRACT

The development of value-added wood-derived polymer products is of significant importance. Of particular interest is the synthesis of advanced bioactive cellulosic materials. In the present research, novel cellulosic honeycomb films are reported. Cellulose was reacted with dimethylthexylsilyl chloride to form regioselective 2,6-di-*O*-thexyldimethylsilyl cellulose followed by substitution of the C3 with functionalized poly(ethylene glycol) (PEG). The free end of the PEG side chains of the regioselective 3-*O*-poly(ethylene glycol)-2,6-di-*O*-thexyldimethylsilyl cellulose served as an attachment point for bioactive molecules. As an example, Fmoc-Gly-OH was linked to the free end of PEG to produce 3-*O*-Fmoc-Gly-poly(ethylene glycol)-2,6-di-*O*-thexyldimethylsilyl cellulose. Honeycomb films were produced through film casting under a humid airflow. AFM analysis revealed the directed self-assembly of the 3-*O*-Fmoc-Gly-poly(ethylene glycol)-2,6-di-*O*-thexyldimethylsilyl cellulose wherein the pendent 3-*O*-Fmoc-Gly-poly(ethylene glycol) groups allocated preferentially around the edges of the honeycomb pores.

© 2013 Elsevier Ltd. All rights reserved.

1. Introduction

Over the last several years the significance of sustainable development has become widely understood and accepted. As a result a growing trend in the research and application of renewable resources has occurred. Cellulose is the most abundant polymer on earth and as such has been extensively studied for the development of advanced materials such as nanocomposites (Goetz, Foston, Mathew, Oksman, & Ragauskas, 2010; Peresin, Habibi, Zoppe, Pawlak, & Rojas, 2010), blood compatible (Liu et al., 2009) and thermally responsive (Azzam, Heux, Putaux, & Jean, 2010; Ifuku & Kadla, 2008) materials. Most recently, particular interest has been in the development of regioselectively substituted cellulose derivatives due to their designable properties, such as solubility and crystallinity (Kondo, Koschella, Heublein, Klemm, & Heinze, 2008). In polysaccharide chemistry, regioselectivity means a pre-set functionalization of one or two selected hydroxyl groups within the repeating unit (Heinze, 2009). 2,2,6,6-Tetramethylpiperidine-1-oxyl radical (TEMPO)-mediated oxidation (Isogai, Saito, & Fukuzumi, 2011) has been extensively applied in functionalizing the primary hydroxyl group at C6 position. Bulky protecting groups such as trityl (Yue & Cowie, 2002),

tert-butyldimethylsilyl (Heinze, Pfeifer, & Petzold, 2008), and thexyldimethylsilyl (Koschella, Heinze, & Klemm, 2001; Petzold, Einfeldt, Gunther, Stein, & Klemm, 2001) groups are often employed in regioselectively modifying cellulose.

Mesoporous and macroporous membranes are receiving considerable research interest, due to their wide range of applications such as separation and dialysis (Risbud & Bhonde, 2001), drug delivery (Ma & McHugh, 2007), electronics (Imada et al., 1999), photonics (Wijnhoven & Vos, 1998), and surfaces for cell growth (Beattie et al., 2006; Stenzel, Barner-Kowollik, & Davis, 2006). Lithography and “stamping” have been applied to deposit biomembranes onto cellulose to form interesting materials with ordered porous structure (Tanaka, Wong, Rehfeldt, Tutus, & Kaufmann, 2004), but they are time-consuming and require special equipment. Simply by placing a thin layer of water in oil (W/O) emulsion in a closed box containing water, honeycomb patterned cellulose acetate films with size of 1–100 μm were formed (Kasai & Kondo, 2004). By means of saponification of the honeycomb films of cellulose triacetate, uniform honeycomb films of cellulose were fabricated by Nemoto et al. (2005) using a three-step transcription method, by which the films could be easily reproduced. Ultrathin (<20 nm) films of poly(methyl methacrylate) (PMMA) with cavities (diameter: 10–160 nm, depth: 1–10 nm) containing cellulose decoration were also reported by using binary polymer blends (Kontturi, Johansson, & Laine, 2009). But the most convenient method to prepare porous films with regular hexagonal arrays, termed

* Corresponding author. Tel.: +1 604 827 5254; fax: +1 604 822 0661.
E-mail address: john.kadla@ubc.ca (J.F. Kadla).

honeycomb structured films and membranes, is to cast films by controlling solvent evaporation under a humid atmosphere, known as “breath figures” (Stenzel, 2002). Specifically during the evaporation of solvent from a polymer solution there is condensation of water onto the cooling surface. By controlling the system the water droplets create an ordered hexagonal template in which the polymer precipitates at the water–solvent interface, resulting in the encapsulation of water droplets and preventing their coalescence (Widawski, Rawiso, & Francois, 1994). Amphiphilicity of polymers is often needed for the formation of honeycomb membranes since the porous micro-structure is coupled with a micro-phase morphology that leads to a hydrophobic surface while the pores are enriched with hydrophilic groups (Wong et al., 2006). Although honeycomb membranes can be formed with either regioselectively or randomly functionalized cellulose derivatives, regioselectively functionalized cellulose derivatives have a more regular molecular structure, so are more suitable for the study of the effect of molecular structure such as the degree of substitution (DS) and the chain length (DP) of the hydrophilic groups on the formation of honeycomb membranes.

It is hypothesized that the poly(ethylene glycol) segments will preferentially interact with the condensing water droplets and act to direct the self-assembly of the regioselective cellulosic honeycomb films. As a result, the attachment of biomolecules to the terminal end of the poly(ethylene glycol) chains would be preferentially allocated to the walls of the honeycomb pores and be accessible to interact with other biomolecules in solution when exposed to water. Not only are some Fmoc-amino acids bioactive with anti-inflammatory activities (Burch et al., 1991), but they are also widely used in the synthesis of peptides when protection of the amino groups is needed (Wu & Xu, 2001). In the present research, Fmoc-Gly-OH was selected as a model amino acid compound to link to the free end of PEG to produce 3-O-Fmoc-Gly-poly(ethylene glycol)-2,6-di-O-thexyldimethylsilyl cellulose. Honeycomb films of 3-O-Fmoc-Gly-poly(ethylene glycol)-2,6-di-O-thexyldimethylsilyl cellulose were cast by controlled solvent evaporation under a humid atmosphere and analyzed using atomic force microscopy (AFM) and a scanning electron microscope (SEM). This work is believed to provide a platform for preparation of bioactive membranes by attaching bioactive molecules for applications such as detection and deactivation of bacteria.

2. Experimental

2.1. Materials

Polyethylene glycol Mw=200 (EG₄), polyethylene glycol Mw=600 (EG₁₃), polyethylene glycol Mw=1000 (EG₂₂), dimethylthexylsilyl chloride (TDMSCI), imidazole, anhydrous N,N-dimethylacetamide (DMA), hydroxybenzotriazole (HOBT), N-(9-fluorenylmethoxycarbonyl)-glycine (Fmoc-Gly-OH), *p*-tosyl chloride, sodium hydride (60% dispersion in mineral oil), N,N'-dicyclohexylcarbodiimide (DCC), 4-(dimethylamino)pyridine (DMAP), sodium sulfite, and tetra-*n*-butylammonium iodide (TBAI) were purchased from Sigma-Aldrich and used as received. Potassium hydroxide, sodium hydroxide, anhydrous magnesium sulfate, potassium iodide, acetone (ACS certified), chloroform (ACS certified), sodium chloride (ACS certified), sodium bicarbonate (ACS certified), and dichloromethane (DCM) were purchased from Fisher Scientific and used as received. Tetrahydrofuran (THF) and anhydrous lithium chloride (Sigma-Aldrich) were dried before use. Cellulose was obtained from the deacetylation of cellulose acetate (average Mn ~30 kDa, Aldrich) using sodium hydroxide in methanol and thoroughly dried prior to use.

2.2. Characterization

¹H and ¹³C NMR spectra were measured using a Bruker AVANCE-300 spectrometer at 25 °C for small molecules and 40 °C for polymers. Chemical shifts were referenced to tetramethyl silane (TMS; 0.0 ppm). Infrared spectra were obtained with a Perkin-Elmer Spectrum One FT-IR spectrometer as potassium bromide pellets in a 3:1 sample to salt ratio (insoluble samples) or as neat films cast from CHCl₃ (soluble samples) onto ZnSe windows. Spectra were recorded at a resolution of 4 cm⁻¹ using a total of 32 scans. Elemental analysis was measured using a Perkin-Elmer Series II CHNS/O analyzer. Polymer molecular weight was determined by using a GPC (Agilent 1100, UV and RI detectors) connected to a multi-angular light scattering detector (DAWN Heleos-II, Wyatt Technologies) and calibrated with polystyrene standards. Columns: Stryagel HR-1, HR-3, and HR-4 (Waters Corp., Milford, USA); temperature: 35 °C, eluting solvent: THF; flowrate: 0.5 mL/min; sample concentration: 2 mg/mL; injection volume: 100 μL. Modulus of honeycomb films was measured by using PeakForce QNM (Quantitative NanoMechanics) mode with AFM (Veeco Multimode coupled with Nanoscope V Controller). The spring constant and deflection sensitivity of a ScanAsyst-Air silicon tip on nitride lever were calibrated with a Sapphire-15M standard (Veeco). The surface morphology of the honeycomb films was observed with AFM and a SEM (Hitachi S-2600N scanning electron microscope). Pore size was measured on SEM images using Image-J software (NIH, USA) and the statistical analysis of pore size distribution was performed based on more than 3000 pores for each sample by means of MATLAB software.

2.3. Synthesis

Poly(ethylene glycol) monotosylate (1a–c) was synthesized from the corresponding poly(ethylene glycol) [Mw = 200 (EG₄) for **1a**, Mw = 600 (EG₁₃) for **1b**, and Mw = 1000 (EG₂₂) for **1c**]. Poly(ethylene glycol) (0.006 mol) was dissolved in 10/40 mL H₂O/THF. Potassium hydroxide (0.34 g, 0.006 mol, 1 equiv.) was added and the solution was cooled in ice water bath. *p*-Tosyl chloride (0.86 g, 0.0045 mol, 0.75 equiv.) solution in 50 mL THF was added dropwise. The reaction mixture was warmed to room temperature and stirred for additional 18 h. The THF was evaporated. Brine solution was added and washed 5 times with chloroform. The organic phases were combined, washed with water, dried over magnesium sulfate and the solvent was removed by evaporation in vacuo. Yield: **1a** 66%; **1b** 77%; **1c** 87%. ¹H NMR (CDCl₃, 300 MHz) (Canaria, Smith, Yu, Fraser, & Lansford, 2005): δ (ppm) 7.69 (d, *J* = 7.89 Hz, 2H), 7.25 (d, *J* = 7.89 Hz, 2H), 4.06 (t, *J* = 4.82 Hz, 2H), 3.7–3.5 (multiplet, 14.5/50.9/87.3H), 2.35 (s, 3H). ¹³C NMR (CDCl₃, 75.4 MHz): (ppm) 144.3, 133.0, 129.4, 127.5 (C₆H₄), 72.2–68.3 (CH₂–EG), 61.3 (CH₂–OH), 21.2 (CH₃–C₆H₄).

Poly(ethylene glycol) monoiodide (2a–c) was synthesized from the corresponding poly(ethylene glycol) monotosylate (**1a–c**). Poly(ethylene glycol) monotosylate (0.006 mol) was dissolved in 50 mL of acetone and carefully added to a refluxing potassium iodide (2.9 g, 0.18 mol, 3 equiv.) in 50 mL of acetone solution. The mixture was refluxed for 18 h and cooled to room temperature. Water was added to receive a clear solution (~50 mL). The acetone was removed under reduced pressure. Saturated sodium sulfite solution (50 mL) was added gaining a colorless solution and the aqueous phase was washed 5 times with chloroform. The organic phases were combined, dried over magnesium sulfate and the solvent was removed by evaporation in vacuo. Yield: **2a** 57%; **2b** 65%; **2c** 98%. ¹H NMR (CDCl₃, 300 MHz): δ (ppm) 3.7–3.5 (multiplet, 14.5/50.9/87.3H), 3.15 (t, 2H). ¹³C NMR (CDCl₃,

75.4 MHz): δ (ppm) 72.1–69.8 ($\text{CH}_2\text{-EG}$), 61.4 ($\text{CH}_2\text{-OH}$), 2.6 ($\text{CH}_2\text{-I}$).

2,6-di-O-thexyldimethylsilyl cellulose (3) (2,6-TDMS cellulose) was synthesized according to the procedure of Koschella et al. (Kadla, Asfour, & Bar-Nir, 2007; Koschella et al., 2001), as reported in the previously published paper (Bar-Nir & Kadla, 2009). Yield: 89%. Elemental analysis: C59.03%, H10.58%. DS: 1.96 (calculated with the data from elemental analysis). Molecular weight: Mw 78 kDa, PDI 1.4. ^1H NMR (C_6D_6 , 313 K, 300 MHz): δ (ppm) 4.77–3.52 (cellulose), 1.86–0.27 (TDMS). ^{13}C NMR (C_6D_6 , 313 K, 75.4 MHz): δ (ppm) 102.5 (C1), 76.9, 75.6, 72.1, 71.9, 60.6 (C6), 35.1 to –2.8 (TDMS).

3-O-hydroxypoly(ethylene glycol)-2,6-di-O-thexyldimethylsilyl cellulose (4a-c) (3-OHPEG-2,6-TDMS cellulose). General procedure: sodium hydride (0.01 mol, 5 equiv.) was washed three times with freshly distilled anhydrous THF. 2,6-TDMS cellulose (**3**) (1 g, 0.002 mol) and tetra-*n*-butylammonium iodide (TBAI) (75 mg, 0.02 mmol, 0.01 equiv.) were added and stirred in 24 mL anhydrous THF, at room temperature for 1 h. Poly(ethylene glycol) monoiodide (**2a-c**) (3.3/7.3/11.3 g, 0.01 mol, 5 equiv.) was added. The mixture was stirred for 72 h at room temperature, and then slowly precipitated into methanol while destroying the excess of sodium hydride. Further purification was done by redissolving the crude polymer in chloroform and precipitating in methanol. Yield: **4a** 0.70 g; **4b** 0.85 g; **4c** 0.60 g. Elemental analysis: **4a** C58.30%, H10.12%; **4c** C58.46%, H10.18%. Molecular weight: **4a** Mw 110 kDa, PDI 1.8; **4c** Mw 160 kDa, PDI 2.8. FT-IR: 3509 (OH), 2957, 2870 (CH_3), 1465, 1378 (CH_2 , CH_3), 1252 (Si-C), 1152, 1117 (Si-O-C), 1078, 1036 (C-O- C_{AGU}), 834, 778 (Si-C/Si-O-C). ^1H NMR (C_6D_6 , 313 K, 300 MHz): δ (ppm) 4.76–3.52 (cellulose), 3.51 (EG), 1.85–0.28 (TDMS). ^{13}C NMR (C_6D_6 , 313 K, 75.4 MHz): δ (ppm) 71.5 (EG), 62.4 (EG- $\text{CH}_2\text{-OH}$), 35.1 to –2.8 (methyl of TDMS).

3-O-Fmoc-Gly-poly(ethylene glycol)-2,6-di-O-thexyldimethylsilyl cellulose (5a-c) (3-AA-PEG-2,6-TDMS cellulose). General procedure: 3-O-hydroxypoly(ethylene glycol)-2,6-di-O-thexyldimethylsilyl cellulose (**4a-c**) (0.0017 mol) was dissolved in 10 mL methylene chloride (DCM). Fmoc-Gly-OH (1.3 g, 0.0043 mol, 2.5 equiv.) and HOBt (0.574 g, 0.0043 mol, 2.5 equiv.) were dissolved in 10 mL DCM and added to the cellulose solution. DMAP (0.020 g, 0.1 equiv.) and DCC (0.7 mL, 0.0043 mol, 2.5 equiv.) were added and the reaction was stirred at room temperature for 8 h. The solution was filtered and concentrated, then precipitated into methanol. Further purification was done by redissolving the crude polymer in chloroform and precipitating in methanol. Yield: **5a** 0.70 g; **5b** 0.84 g; **5c** 0.62 g. Elemental analysis: **5a** C59.57%, H9.80%, N0.42%; **5b** C59.28%, H9.87%, N0.36%; **5c** C58.99%, H9.86%, N0.33%. Degree of substitution calculated with the nitrogen content from the elemental analysis: **5a** 0.16; **5b** 0.15; **5c** 0.15. Molecular weight: **5a** Mw 95 kDa, PDI 1.4; **5b** Mw 100 kDa, PDI 1.6; **5c** Mw 97 kDa, PDI 2.2. FT-IR: 3503 (OH), 2957, 2870 (CH_3), 1760 ($-\text{CH}_2\text{-COO}-$), 1732 ($-\text{NH-COO}-$), 1515 (amide II band) (Socrates, 2001), 1465, 1378 (CH_2 , CH_3), 1252 (Si-C), 1152, 1118 (Si-O-C), 1079, 1036 (C-O- C_{AGU}), 834, 778 (Si-C/Si-O-C). ^{13}C NMR (C_6D_6 , 313 K, 75.4 MHz): δ = 145.0, 142.2, 125.9, 120.6, 76.2, 71.4, 69.4, 67.4, 64.7, 48.1, 43.4, 35.1 to –2.8 (TDMS).

2.4. Film preparation

Honeycomb-patterned films were prepared by applying 10 μL of neat solution (1% in toluene) onto a glass slide in a humid environment (flow rate: 700 mL/min; relative humidity: 70–80%; room temperature).

3. Results and discussion

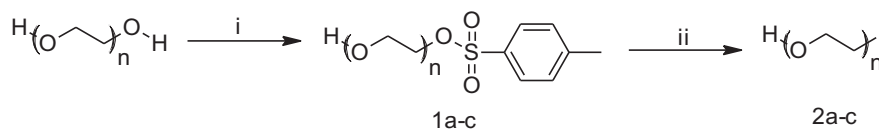
3.1. Synthesis and characterization of poly(ethylene glycol) monoiodide

In order to synthesize 3-AA-PEG-2,6-TDMS cellulose, poly(ethylene glycol) monoiodide (**2a-c**) was first synthesized. The reaction scheme for the preparation of poly(ethylene glycol) monoiodide is illustrated in Scheme 1. Poly(ethylene glycol) monotosylate (**1a-c**) was synthesized by reacting poly(ethylene glycol) with *p*-tosyl chloride at room temperature for 18 h, followed by further conversion to poly(ethylene glycol) monoiodide (**2a-c**) by reacting **1a-c** with potassium iodide.

The synthesized products were characterized with NMR. ^1H and ^{13}C NMR spectra of the synthesized poly(ethylene glycol) monotosylate **1b** and poly(ethylene glycol) monoiodide **2b**, as well as the purchased poly(ethylene glycol) Mw=600 (EG₁₃) are compared in Figs. 1 and 2, respectively. As seen in Fig. 1, in contrast to the spectrum of the starting material poly(ethylene glycol), additional peaks at 7.69, 7.25, 4.06, and 2.35 ppm of the product **1b** indicate successful introduction of tosyl groups at the end of poly(ethylene glycol). Although the reaction stoichiometry was selected to functionalize only one of the hydroxyl groups, a small amount (ca. 5%, see supporting information) of poly(ethylene glycol) di-tosylate was formed and some unreacted poly(ethylene glycol) remained after the reaction. The unreacted poly(ethylene glycol) was removed through washing. Complete conversion of **1b** to **2b** was confirmed by the disappearance of the above mentioned tosyl-related peaks and the appearance of the new peak of **2b** at 3.15 ppm. According to Fig. 2, the introduction of tosyl group to the end of poly(ethylene glycol) was also evidenced by the new appearance of tosyl peaks (**1b**) at 144.3, 133.0, 129.4, 127.5, and 21.2 ppm compared to the spectrum of poly(ethylene glycol). After the conversion of **1b** to **2b**, these tosyl-related peaks disappeared and a new peak appeared at 2.6 ppm due to replacement of the tosyl group with an iodo group. The unreacted hydroxyl group at the other end of **1b** and **2b** was confirmed by the peak at 61.4 ppm.

3.2. Synthesis and characterization of 3-AA-PEG-2,6-TDMS cellulose

By using the synthesized poly(ethylene glycol) monoiodide (**2a-c**), 3-O-Fmoc-Gly-poly(ethylene glycol)-2,6-di-O-thexyldimethylsilyl cellulose was then synthesized. Scheme 2 displays the synthetic scheme of 3-O-Fmoc-Gly-poly(ethylene glycol)-2,6-di-O-thexyldimethylsilyl cellulose. The regenerated cellulose (from cellulose acetate, average Mn 30 kDa) was employed in this research because it has known and relatively low molecular weight. Cellulose derivatives of lower molecular weight should have better solubility for chemical reaction and film casting. The regenerated cellulose is not soluble in common solvents but can be dissolved in DMA/LiCl. After the silylation of cellulose, the formed product can be easily dissolved in many solvents including THF, chloroform, toluene, benzene, etc. By reacting cellulose with TDMSCl in DMA/LiCl in the presence of imidazole at 100 °C, silylation of cellulose took place preferentially at the C6 and C2 positions (Koschella et al., 2001). The bulky TDMS groups bonded to the C6 and C2 positions prevented the less reactive hydroxyl group at the C3 position from being further silylated, resulting in regioselective protection of the hydroxyl groups of cellulose. Poly(ethylene glycol) monoiodide (**2a-c**) was then attached to the C3 position at the regioselective 2,6-TDMS cellulose (**3**) to generate 3-OHPEG-2,6-TDMS cellulose (**4a-c**), with which Fmoc-Gly-OH was subsequently reacted to afford 3-O-Fmoc-Gly-poly(ethylene glycol)-2,6-di-O-thexyldimethylsilyl cellulose (**5a-c**).



Scheme 1. Synthetic scheme to poly(ethylene glycol) monoiodide. Note: $n = 4$ for **a**, $n = 13$ for **b**, and $n = 22$ for **c**. (i) *p*-Tosyl chloride, KOH, THF, H₂O, room temperature, 18 h; (ii) KI, acetone, refluxing, 18 h.

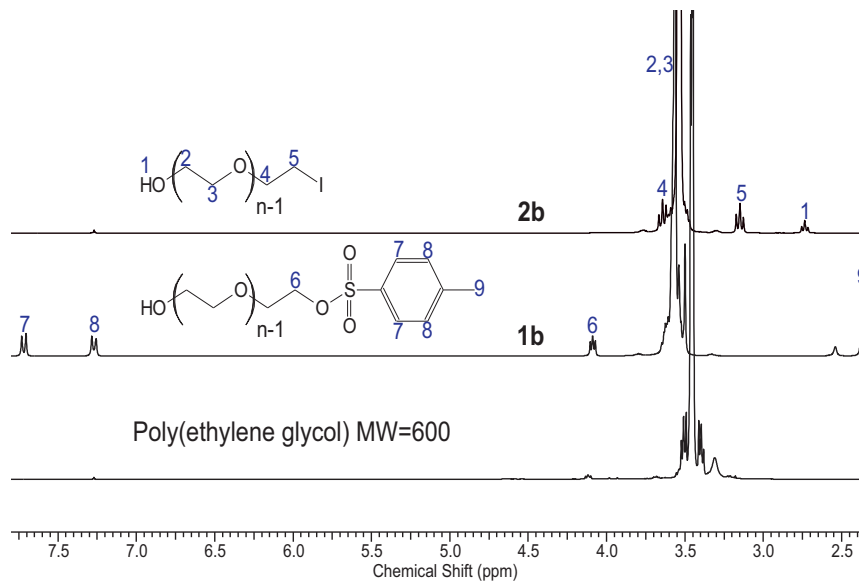


Fig. 1. A comparison of ¹H NMR spectra of poly(ethylene glycol) Mw = 600, and the synthesized poly(ethylene glycol) monotosylate (**1b**) and poly(ethylene glycol) monoiodide (**2b**).

The synthesized cellulose derivatives were characterized with FTIR, ¹H and ¹³C NMR, and elemental analysis. The characterization results of product **3** have been previously reported (Bar-Nir & Kadla, 2009). Fig. 3 displays a comparison of ¹H NMR spectra of the synthesized products **3**, **4b**, and **5b**. In contrast to the ¹H NMR spectrum of 2,6-TDMS cellulose, the additional peak in the spectrum of **4b** appearing at 3.51 ppm suggests successful attachment of poly(ethylene glycol) to the C3 position of 2,6-TDMS cellulose. It

should be noted that the small amount of impurity, poly(ethylene glycol) di-tosylate, could act as a crosslink agent to bond different cellulose chains together. However, the effect of crosslink is very limited as the formed insoluble crosslinked products during the synthesis of **4a–c** would be filtered off during the purification process after the reaction. In the previous work (Bar-Nir & Kadla, 2009), iodide of poly(ethylene glycol) monomethyl ether was attached to the C3 position of 2,6-TDMS cellulose, resulting

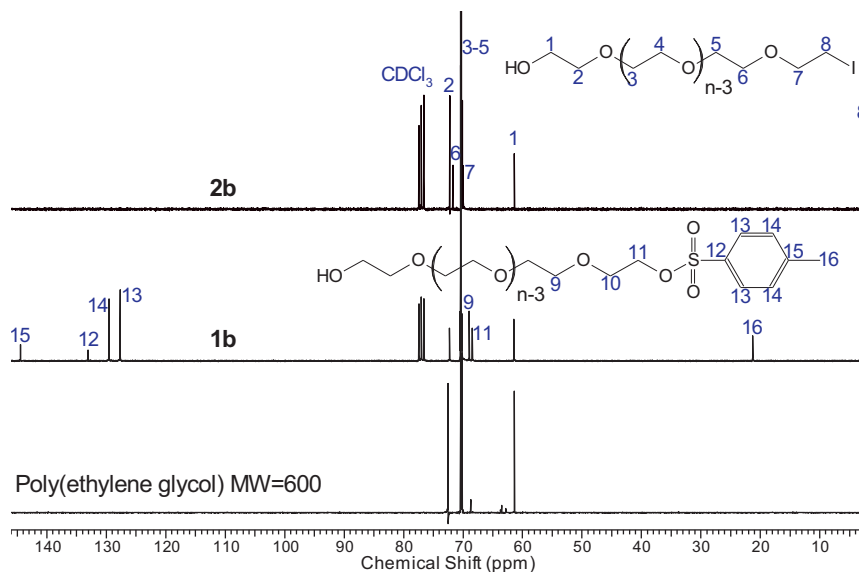
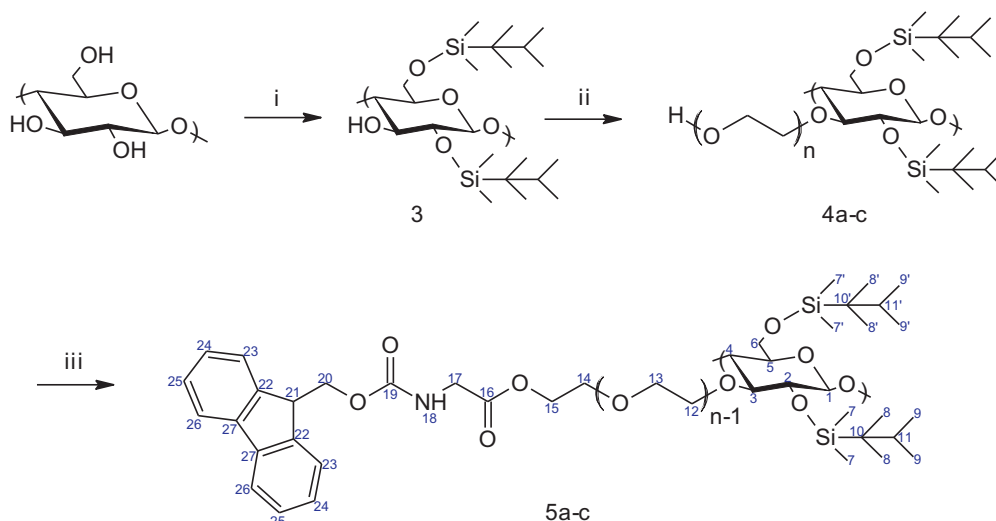


Fig. 2. A comparison of ¹³C NMR spectra of poly(ethylene glycol) Mw = 600, and the synthesized poly(ethylene glycol) monotosylate (**1b**) and poly(ethylene glycol) monoiodide (**2b**).



Scheme 2. Synthetic scheme to 3-O-Fmoc-Gly-poly(ethylene glycol)-2,6-di-O-thexyldimethylsilyl cellulose. Note: $n=4$ for **a**, $n=13$ for **b**, and $n=22$ for **c**. (i) TDMSCl, imidazole, DMA, LiCl; (ii) poly(ethylene glycol) monoiodide **2a-c**, NaH, TBAI, THF; (iii) Fmoc-Gly-OH, HOBT, DMAP, DCC, DCM, room temperature, 8 h.

in relatively high DS 3-O-methoxypoly(ethylene glycol)-2,6-di-O-thexyldimethylsilyl cellulose. In order to link Fmoc-Gly-OH to the free end of PEG at the C3 position of 2,6-TDMS cellulose, poly(ethylene glycol) monoiodide (**2a-c**) was employed in the synthesis of **4a-c**. The relatively low DS of **4a-c** and thus **5a-c** may be due to the side reactions of intramolecular and intermolecular elimination of **2a-c** during the synthesis of **4a-c**. In addition, it could not be excluded that **2a-c** reacted with itself to increase the side chain length during the synthesis of **4a-c**, but according to the integration analysis of the ^1H NMR spectrum of product **5b** in CD_2Cl_2 (see supporting information), this reaction should be insignificant. The additional peaks at 7.58, 7.43, and 7.21 ppm in the spectrum of **5b** are attributed to the aromatic group, indicating successful linkage of Fmoc-Gly-OH to the free end of PEG at the C3 position of 2,6-TDMS cellulose.

The successful synthesis of **5a-c** was also confirmed by ^{13}C NMR and FTIR. As seen in Fig. 4, by attaching poly(ethylene glycol) to 2,6-TDMS cellulose (**3**), additional ^{13}C peaks of product **4b** appear at 62.4 and 71.4 ppm, attributed to the end methylene

($-\text{CH}_2-\text{CH}_2-\text{OH}$) and other methylene groups in the PEG side chain, respectively. After the reaction of **4b** with Fmoc-Gly-OH, the peak at 62.4 ppm disappears and many new ^{13}C NMR peaks appear at 145.0, 142.2, 125.9, 120.6, 69.4, 67.4, 64.7, 48.1, and 43.4 ppm in the spectrum of the formed product **5b** (Fig. 4). The assignment of these peaks is shown in Fig. 4. The peaks of aromatic carbons at positions 24 and 25 (Scheme 2) are overlapped with the solvent (C_6D_6) peaks; hence they could not be assigned. The disappearance of the peak at 62.4 ppm indicates the reaction of the end hydroxyl group at the free end of PEG side chain. In addition, FTIR results suggest successful conversion of **4b** to **5b** by the additional carbonyl peaks at 1760 and 1732 cm^{-1} and the peak at 1515 cm^{-1} of sample **5b**.

3.3. Formation of honeycomb membrane from 3-AA-PEG-2,6-TDMS cellulose

In contrast to the top-down techniques such as the lithographic method to form micro-sized patterns, bottom-up techniques are

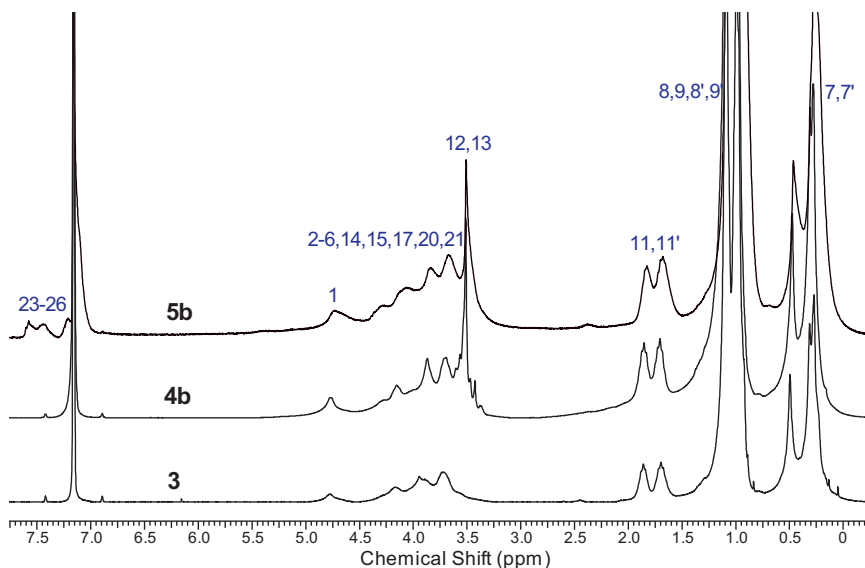


Fig. 3. A comparison of ^1H NMR spectra of the synthesized products of 2,6-TDMS-cellulose (**3**), 3-OHPEG-2,6-TDMS cellulose (**4b**), and 3-AA-PEG-2,6-TDMS cellulose (**5b**) (see Scheme 2 for the labeling).

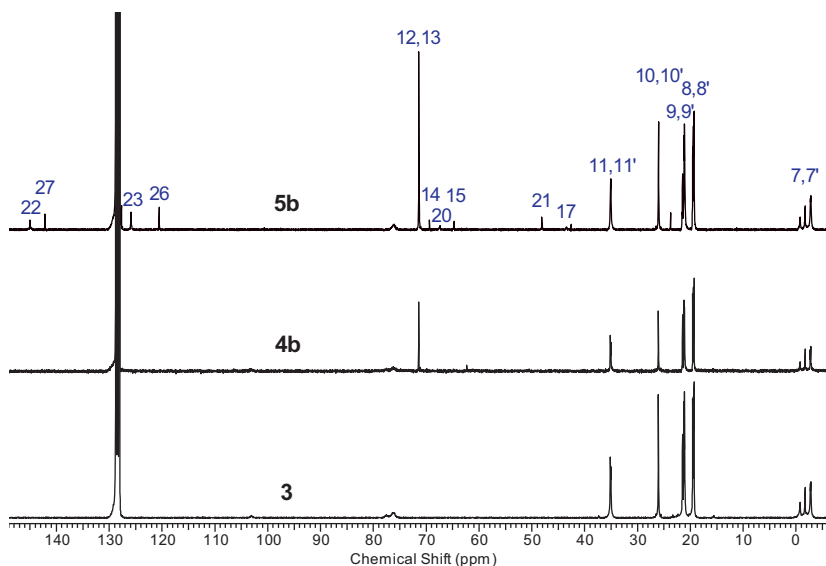


Fig. 4. A comparison of ^{13}C NMR spectra of the synthesized products of 2,6-TDMS-cellulose (**3**), 3-OHPEG–2,6-TDMS cellulose (**4b**), and 3-AA-PEG–2,6-TDMS cellulose (**5b**) (see Scheme 2 for the labeling).

often applied to form honeycomb structured porous materials. Wong et al. (2006) investigated the four different casting variations of the water droplet templating method, i.e., airflow, cold stage, casting on water, and emulsion, and found that the airflow casting technique was a versatile method for many polymer materials. In addition to many physical parameters such as humidity and airflow rate, chemical aspect is a major factor to affect the formation of regular honeycomb-patterned films (Wong, Davis, Barner-Kowollik, & Stenzel, 2007). Our synthesized amphiphilic 3-AA-PEG–2,6-TDMS celluloses were cast under a humid airflow to form honeycomb films. A schematic diagram of the formation of honeycomb films with the “breath figures” method is shown in Fig. 5. When a thin layer of polymer solution was placed under a humid air flow, the decreasing temperature of the polymer solution due to evaporation of the solvent resulted in condensation of water droplets onto the surface of polymer solution. With the solvent further evaporating, the water droplets were rearranged to form an ordered hexagonal template by capillary force. Honeycomb films were formed with precipitation of the polymer at the water–solvent interface and complete evaporation of the solvent and water. Fig. 6 displays the surface profiles with height (Fig. 6a) and modulus (Fig. 6b) skins for

the honeycomb films from the product **5b**, respectively. Quantitative nanomechanical analysis of the surfaces (Fig. 6b) reveals a clear difference in the modulus along the edge of the pores (red region) as compared to that along the main skeleton between the pores (yellow region). As seen in Fig. 6c, the moduli vary from ca. 100 MPa at the edges of the pores to ca. 400 MPa at the regions between the pores. The larger modulus on the main skeleton is in good agreement with that found for TDMS cellulose films (see supporting information). Because the PeakForce QNM mode of AFM is not applicable for liquids or waxes, the modulus of the PEG oligomers (EG₄, EG₁₃, and EG₂₂) could not be measured for comparison. These findings indicate that when honeycomb membranes are formed via the “breath figures” method, the condensed water droplets seem to interact with the hydrophilic groups in the macromolecule, i.e., PEG side chain and results in a preferential allocation of the softer hydrophilic PEG chains around the pores.

Further evidence of the preferential allocation of the PEG groups around the edges of the honeycomb pores was apparent from AFM analysis of the honeycomb films in water. Fig. 7 shows AFM images of the honeycomb membrane in air (Fig. 7A) and after the addition of water (Fig. 7B). The image obtained using the liquid clearly shows

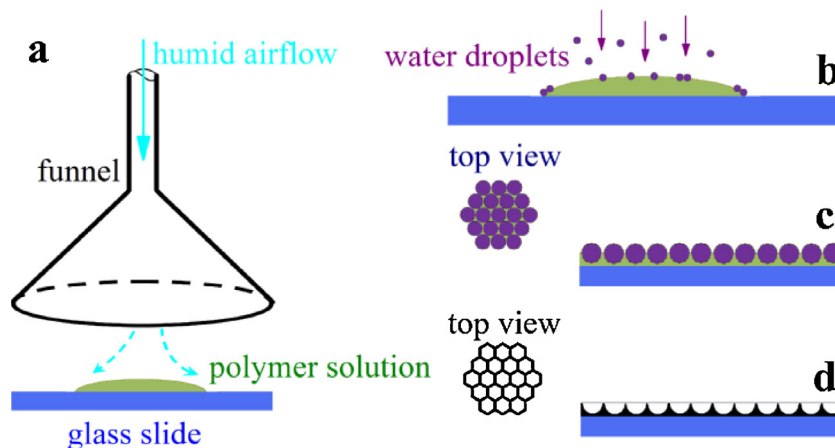


Fig. 5. A schematic diagram of the formation of honeycomb films: (a) exposure of a thin layer of polymer solution under humid air flow; (b) condensation of water droplets onto the cooling surface of the polymer solution due to evaporation of the solvent; (c) rearrangement of the water droplets to form an ordered hexagonal template resulting from the capillary force; (d) precipitation of the polymer at the water–solvent interface to form honeycomb films after complete evaporation of the solvent and water.

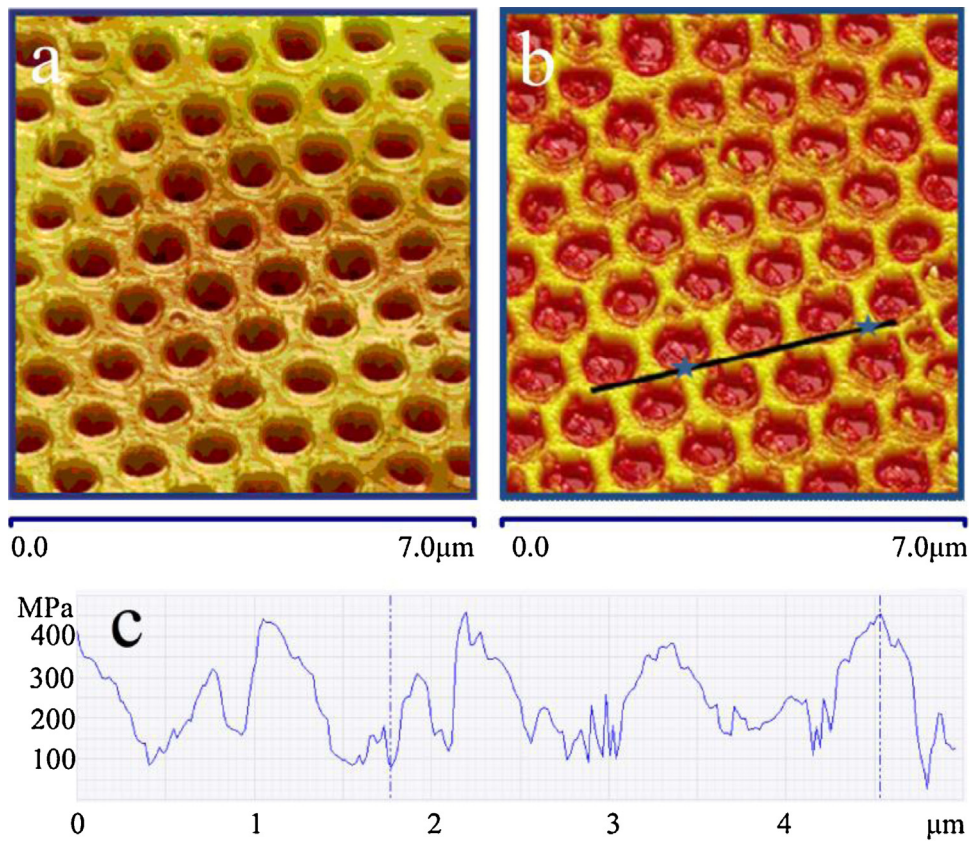


Fig. 6. AFM images of honeycomb membrane from the synthesized product **5b**. (a) 3D height skin; (b) 3D modulus skin; (c) modulus profile along the black line in (b). (For interpretation of the references to color in this figure legend, the reader is referred to the web version of this article.)

that the morphology of the membrane surface changes upon exposure to water. As the polymer is not soluble in water, this observed phenomenon is due to mobilization of the hydrophilic PEG side chains rather than the hydrophobic skeleton.

As observed by Kontturi et al. (2011), molecular rearrangements occurred during exposure of the regenerated cellulose film to water due to its hydrophilicity. When water penetrates the amphiphilic polymer chains, the hydrophilic part, i.e., PEG side chains, interact with water to move to energetically more favorable positions and conformations and the resulting film morphology should be different from the initial state. During the casting of the membrane, the

hydrophilic PEG side chains were limited to interact with micro-sized water droplets. When the formed honeycomb membrane was exposed to water, the PEG side chains were no longer limited to be around the pores; hence the PEG side chains extend out from the regular pores. This “activation” or “mobilization” of the PEG side chains upon exposure to water could be of significant importance in the development and utilization of such materials as bioactive films and membranes.

In addition to AFM, the formed honeycomb films from products **5a**, **5b**, and **5c** were also examined with SEM. The images and pore size distribution histograms are displayed in Fig. 8. It was found that

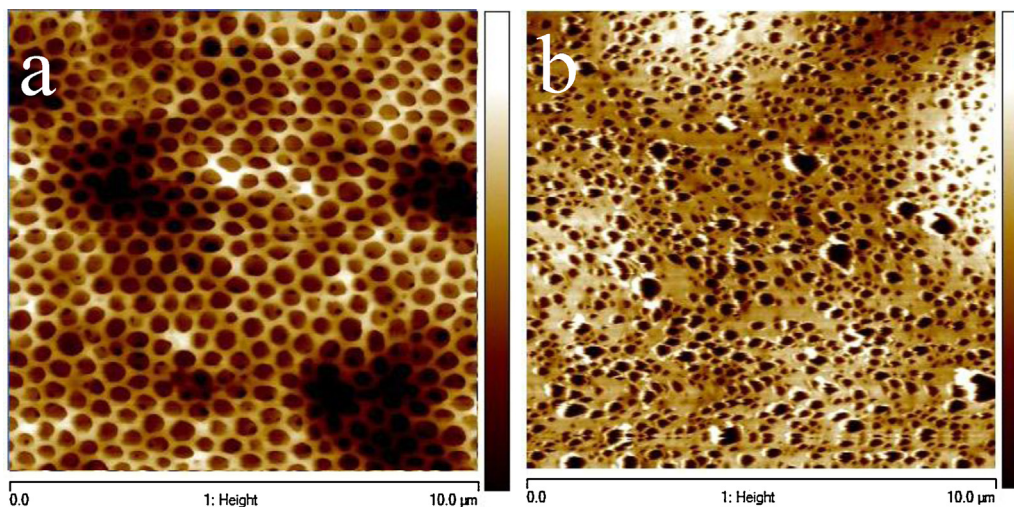


Fig. 7. AFM images of the honeycomb membrane from product **5b** in air (a) and in water (b).

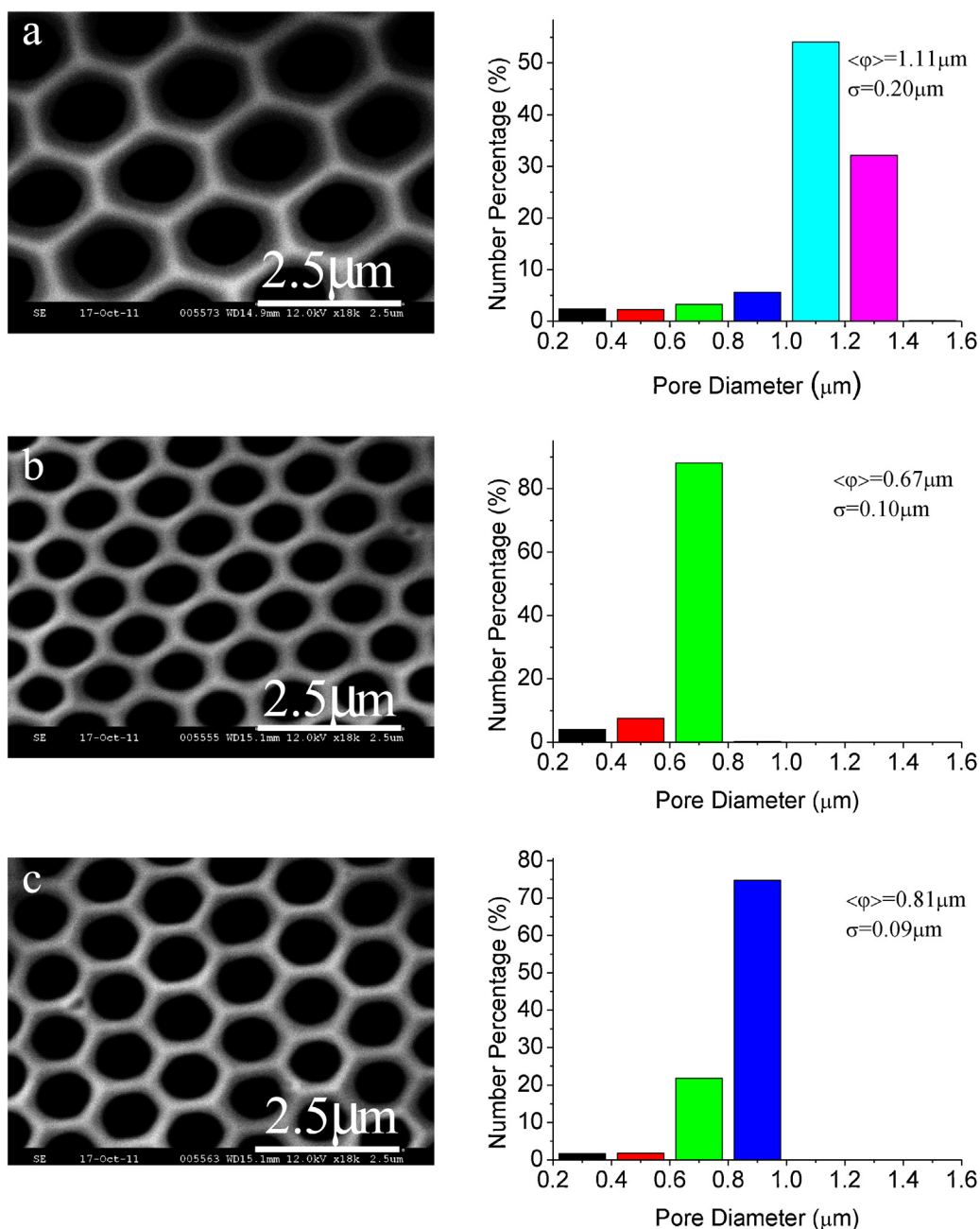


Fig. 8. SEM images and pore size distribution histograms of honeycomb films of samples **5a**, **5b** and **5c** cast at a concentration of 1% in toluene.

the films from products **5b** and **5c** had more narrow distribution (standard deviation: 0.10 and 0.09 μm, respectively) and smaller pore size (average pore diameter: 0.67 and 0.81 μm, respectively) than that from **5a** (standard deviation: 0.20 μm, average pore diameter: 1.11 μm). Work is underway to investigate the effect of PEG side chain length, degree of substitution, and casting conditions on honeycomb film formation and properties.

4. Conclusions

Poly(ethylene glycol) monoiodide of three different lengths was synthesized and attached to the C3 position of the regioselective 2,6-TDMS cellulose to afford an amphiphilic polymer. The free hydroxyl end of the PEG side chains was successfully linked an amino acid, Fmoc-Gly-OH and the formed 3-*O*-Fmoc-Gly-poly(ethylene glycol)-2,6-di-*O*-hexyldimethylsilyl cellulose was cast using the “breath figures” method to form

honeycomb-patterned films. Directed self-assembly and preferential allocation of the hydrophilic PEG chains by interaction with water was confirmed by AFM. Exposure of these films to water revealed that the PEG side chains became “activated” or “mobilized”. The length of the hydrophilic PEG chains showed a significant effect on the pore size and the pore size distribution of the formed honeycomb films. These materials illustrate the potential for the development of bioactive cellulosic materials wherein immobilized biomolecules can be preferentially allocated to the pore region of the honeycomb-patterned films and can be “activated” to interact with molecules in solution.

Acknowledgment

The authors appreciate financial support by the SENTINEL bioactive paper network.

Appendix A. Supplementary data

Supplementary data associated with this article can be found, in the online version, at <http://dx.doi.org/10.1016/j.carbpol.2012.12.076>.

References

- Azzam, F., Heux, L., Putaux, J.-L., & Jean, B. (2010). Preparation by grafting onto, characterization, and properties of thermally responsive polymer-decorated cellulose nanocrystals. *Biomacromolecules*, *11*(12), 3652–3659.
- Bar-Nir, B. B.-A., & Kadla, J. F. (2009). Synthesis and structural characterization of 3-O-ethylene glycol functionalized cellulose derivatives. *Carbohydrate Polymers*, *76*(1), 60–67.
- Beattie, D., Wong, K. H., Williams, C., Poole-Warren, L. A., Davis, T. P., Barner-Kowollik, C., et al. (2006). Honeycomb-structured porous films from polypyrrole-containing block copolymers prepared via RAFT polymerization as a scaffold for cell growth. *Biomacromolecules*, *7*(4), 1072–1082.
- Burch, R. M., Weitzberg, M., Blok, N., Muhlhauser, R., Martin, D., Farmer, S. G., et al. (1991). N-(Fluorenyl-9-methoxycarbonyl) amino acids, a class of antiinflammatory agents with a different mechanism of action. *Proceedings of the National Academy of Sciences of the United States of America*, *88*(2), 355–359.
- Canaria, C. A., Smith, J. O., Yu, C. J., Fraser, S. E., & Lansford, R. (2005). New syntheses for 11-(mercaptoundecyl)triethylene glycol and mercaptododecyltriethyleneoxy biotin amide. *Tetrahedron Letters*, *46*(28), 4813–4816.
- Goetz, L., Foston, M., Mathew, A. P., Oksman, K., & Ragauskas, A. J. (2010). Poly(methyl vinyl ether-co-maleic acid)-polyethylene glycol nanocomposites cross-linked in situ with cellulose nanowhiskers. *Biomacromolecules*, *11*(10), 2660–2666.
- Heinze, T. (2009). Hot topics in polysaccharide chemistry – selected examples. *Macromolecular Symposia*, *280*(1), 15–27.
- Heinze, T., Pfeifer, A., & Petzold, K. (2008). Functionalization pattern of tert-butylidimethylsilyl cellulose evaluated by NMR spectroscopy. *Bioresources*, *3*(1), 79–90.
- Ifuku, S., & Kadla, J. F. (2008). Preparation of a thermosensitive highly regioselective cellulose/N-isopropylacrylamide copolymer through atom transfer radical polymerization. *Biomacromolecules*, *9*(11), 3308–3313.
- Imada, M., Noda, S., Chutinan, A., Tokuda, T., Murata, M., & Sasaki, G. (1999). Coherent two-dimensional lasing action in surface-emitting laser with triangular-lattice photonic crystal structure. *Applied Physics Letters*, *75*(3), 316–318.
- Isogai, A., Saito, T., & Fukuzumi, H. (2011). TEMPO-oxidized cellulose nanofibers. *Nanoscale*, *3*(1), 71–85.
- Kadla, J. F., Asfour, F. H., & Bar-Nir, B. (2007). Micropatterned thin film honeycomb materials from regiospecifically modified cellulose. *Biomacromolecules*, *8*(1), 161–165.
- Kasai, W., & Kondo, T. (2004). Fabrication of honeycomb-patterned cellulose films. *Macromolecular Bioscience*, *4*(1), 17–21.
- Kondo, T., Koschella, A., Heublein, B., Klemm, D., & Heinze, T. (2008). Hydrogen bond formation in regioselectively functionalized 3-mono-O-methyl cellulose. *Carbohydrate Research*, *343*(15), 2600–2604.
- Kontturi, E., Johansson, L.-S., & Laine, J. (2009). Cellulose decorated cavities on ultrathin films of PMMA. *Soft Matter*, *5*(9), 1786–1788.
- Kontturi, E., Suchy, M., Penttila, P., Jean, B., Pirkkalainen, K., Torkkeli, M., et al. (2011). Amorphous characteristics of an ultrathin cellulose film. *Biomacromolecules*, *12*(3), 770–777.
- Koschella, A., Heinze, T., & Klemm, D. (2001). First synthesis of 3-O-functionalized cellulose ethers via 2,6-di-O-protected silyl cellulose. *Macromolecular Bioscience*, *1*(1), 49–54.
- Liu, P.-S., Chen, Q., Liu, X., Yuan, B., Wu, S.-S., Shen, J., et al. (2009). Grafting of zwitterion from cellulose membranes via ATRP for improving blood compatibility. *Biomacromolecules*, *10*(10), 2809–2816.
- Ma, D., & McHugh, A. J. (2007). The interplay of phase inversion and membrane formation in the drug release characteristics of a membrane-based delivery system. *Journal of Membrane Science*, *298*(1–2), 156–168.
- Nemoto, J., Uraki, Y., Kishimoto, T., Sano, Y., Funada, R., Obata, N., et al. (2005). Production of mesoscopically patterned cellulose film. *Bioresource Technology*, *96*(17), 1955–1958.
- Peresin, M. S., Habibi, Y., Zoppe, J. O., Pawlak, J. J., & Rojas, O. J. (2010). Nanofiber composites of polyvinyl alcohol and cellulose nanocrystals: Manufacture and characterization. *Biomacromolecules*, *11*(3), 674–681.
- Petzold, K., Einfeldt, L., Gunther, W., Stein, A., & Klemm, D. (2001). Regioselective functionalization of starch: Synthesis and ¹H NMR characterization of 6-O-silyl ethers. *Biomacromolecules*, *2*(3), 965–969.
- Risbud, M. V., & Bhonde, R. R. (2001). Suitability of cellulose molecular dialysis membrane for bioartificial pancreas: In vitro biocompatibility studies. *Journal of Biomedical Materials Research*, *54*(3), 436–444.
- Socrates, G. (2001). *Infrared and Raman characteristic group frequencies: Tables and charts*. Chichester, England: John Wiley & Sons Ltd.
- Stenzel, M. H. (2002). Formation of regular honeycomb-patterned porous film by self-organization. *Australian Journal of Chemistry*, *55*(4), 239–243.
- Stenzel, M. H., Barner-Kowollik, C., & Davis, T. P. (2006). Formation of honeycomb-structured, porous films via breath figures with different polymer architectures. *Journal of Polymer Science Part A: Polymer Chemistry*, *44*(8), 2363–2375.
- Tanaka, M., Wong, A. P., Rehfeldt, F., Tutus, M., & Kaufmann, S. (2004). Selective deposition of native cell membranes on biocompatible micropatterns. *Journal of the American Chemical Society*, *126*(10), 3257–3260.
- Widawski, G., Rawiso, M., & Francois, B. (1994). Self-organized honeycomb morphology of star-polymer polystyrene films. *Nature*, *369*(6479), 387–389.
- Wijnhoven, J. E. G. J., & Vos, W. L. (1998). Preparation of photonic crystals made of air spheres in titania. *Science*, *281*(5378), 802.
- Wong, K., Hernández-Guerrero, M., Granville, A., Davis, T., Barner-Kowollik, C., & Stenzel, M. (2006). Water-assisted formation of honeycomb structured porous films. *Journal of Porous Materials*, *13*(3), 213–223.
- Wong, K. H., Davis, T. P., Barner-Kowollik, C., & Stenzel, M. H. (2007). Honeycomb structured porous films from amphiphilic block copolymers prepared via RAFT polymerization. *Polymer*, *48*(17), 4950–4965.
- Wu, Y., & Xu, J.-C. (2001). Synthesis of chiral peptide nucleic acids using Fmoc chemistry. *Tetrahedron*, *57*(38), 8107–8113.
- Yue, Z., & Cowie, J. M. G. (2002). Preparation and chiroptical properties of a regioselectively substituted cellulose ether with PEO side chains. *Macromolecules*, *35*(17), 6572–6577.